

## Threat learning in space: how stimulus-outcome spatial compatibility modulates conditioned skin conductance response<sup>☆</sup>

F. Starita<sup>a,\*</sup>, Y. Stussi<sup>b,c</sup>, S. Garofalo<sup>a</sup>, G. di Pellegrino<sup>a</sup>

<sup>a</sup> Center for Studies and Research in Cognitive Neuroscience, Department of Psychology, University of Bologna, 40126 Bologna, Italy

<sup>b</sup> Department of Psychology, Harvard University, Cambridge, MA 02138, USA

<sup>c</sup> Swiss Center for Affective Sciences & Department of Psychology, University of Geneva, Geneva, Switzerland

### ARTICLE INFO

#### Keywords:

Pavlovian conditioning  
Fear learning  
Spatial compatibility  
Rescorla-Wagner  
Computational modeling

### ABSTRACT

A central question in Pavlovian conditioning concerns the critical conditions that drive the acquisition and maintenance of the stimulus-outcome association. The spatial relationship between the conditioned (CS) and unconditioned (US) stimuli is considered to exert strong effects on learning. However, how spatial information modulates Pavlovian learning remains mostly unexplored in humans. Here, we test how the compatibility between the CS and the US location influences the acquisition, extinction, and recovery (following reinstatement) of Pavlovian conditioned threat. Participants ( $N = 20$ ) completed a differential threat conditioning task in which visual CSs appeared on the same (compatible) or opposite (incompatible) hemispace as the US delivery (aversive shock to one hand), while their skin conductance response served as an index of learning. Results show that initial threat expectations were biased in favor of compatible CSs before conditioning. Nevertheless, this bias was revised during acquisition to reflect current stimulus-outcome contingencies. Computational modeling suggested that this effect occurred through a higher reliance on positive aversive prediction errors for incompatible CSs, thereby facilitating learning of their association with the US. Additionally, the conditioned response to incompatible CSs was associated with initially slower extinction and a greater recovery after threat reinstatement. These findings suggest that spatial information conveyed by stimuli and outcomes can be flexibly used to enact defensive responses to the current source of danger, highlighting the adaptive nature of Pavlovian learning.

Pavlovian threat (“fear”) conditioning is an adaptive form of learning that enables organisms to anticipate and avoid potential threat. During threat conditioning, conditioned stimuli (CSs) gain (or update their) motivational significance through pairing with an aversive outcome (i. e., unconditioned stimulus, US), thereby becoming warning cues for impending threat and eliciting changes in physiological response, subjective experience, and behavior, referred to as the conditioned response. A central question in Pavlovian conditioning concerns the critical conditions that drive the acquisition and maintenance of the stimulus-outcome association (e.g., Delamater, 2012; Li and McNally, 2014; Nasser and Delamater, 2016; Rescorla, 1988). For example, the

temporal relationship between CS presentation and US delivery is known to influence how efficiently organisms learn CS-US associations, such that the closer in time the CS and the US occur, the more likely they will become associated (e.g., Mackintosh, 1974). Indeed, Pavlovian conditioning tasks in which the CS and the US overlap in time (e.g., delay conditioning) lead to greater conditioning than tasks wherein the CS and the US are separated by a time interval (e.g., trace conditioning; see, e.g., Bouton, 2007; Kirkpatrick and Balsam, 2016). In a similar vein, the spatial relationship between the CS and the US has been suggested to influence Pavlovian conditioning, such that learning may be facilitated the closer in space the CS and the US are (see Nasser and Delamater,

<sup>☆</sup> The authors would like to thank Luigi Degni, Valentina Degli Esposti and Daniela Dalbagnò for their assistance with data collection. F.S. is supported by a Bial Foundation Grant for Scientific Research 2020/2021 [Grant Number 47/20]. Y.S. was supported by an Early Postdoc.Mobility fellowship (P2GEP1\_187911) from the Swiss National Science Foundation. Work supported by #NEXTGENERATIONEU (NGEU) and funded by the Ministry of University and Research (MUR), National Recovery and Resilience Plan (NRRP), project MNESYS (PE00000006) – A Multiscale integrated approach to the study of the nervous system in health and disease (DN. 1553 11.10.2022). The authors declare no conflict of interest. Data and code related to the manuscript are publicly available on <https://osf.io/cds4k/>

\* Corresponding author at: Center for Studies and Research in Cognitive Neuroscience, Department of Psychology, University of Bologna, Viale Rasi e Spinelli, 176, 47521 Cesena (FC), Italy.

E-mail address: [francesca.starita2@unibo.it](mailto:francesca.starita2@unibo.it) (F. Starita).

<https://doi.org/10.1016/j.ijpsycho.2023.06.003>

Received 26 January 2023; Received in revised form 14 April 2023; Accepted 4 June 2023

Available online 7 June 2023

0167-8760/© 2023 The Authors. Published by Elsevier B.V. This is an open access article under the CC BY-NC-ND license (<http://creativecommons.org/licenses/by-nc-nd/4.0/>).

2016; see also Christie, 1996; Rescorla and Cunningham, 1979). Nevertheless, while the effects of changes in CS-US temporal relationship on learning have been extensively studied (see Kirkpatrick and Balsam, 2016), how variations in CS-US spatial relationship affect Pavlovian threat conditioning remains mostly unexplored (Nasser and Delamater, 2016).

In humans, a few studies have investigated the role of CS-US spatial relationship on Pavlovian threat conditioning by manipulating CS proximity to participants' body, where the US was delivered (Åhs et al., 2015; Faul et al., 2020; Rosén et al., 2017, 2019), leading to mixed results overall. In fact, the acquisition of threat conditioning was found to be facilitated either for proximal CSs (i.e., closer to the US) (Faul et al., 2020) or for distal CSs (i.e., farther away from the US) (Rosén et al., 2017, 2019). Similarly, proximal CSs have shown enhanced resistance to extinction in some studies (Åhs et al., 2015; Faul et al., 2020), but not in others (Rosén et al., 2017, 2019). Additionally, Zhang et al. (2016) tested whether the laterality of the US delivery on the body would affect the acquisition of threat conditioning, thus presenting different CSs that predicted a US either to the left or right arm (e.g., red circle/right arm US, blue circle/left arm US). They found that while skin conductance response and facial electromyography during CSs presentation were not affected by the laterality of impending US, electromyographic response was greater in the arm in which the US was predicted relative to the contralateral arm. Although these findings suggest that spatial information can modulate threat conditioning, the role of the spatial relationship between the CS and the US remains open for investigation.

Here, we aim to further examine how spatial information influences Pavlovian learning. To do so, we extend the research on threat conditioning and spatial information by keeping CSs' proximity to the body constant and investigating spatial information in terms of CS-US compatibility. Specifically, we test whether threat conditioning is sensitive to the compatibility between the location of stimulus appearance and that of outcome delivery (e.g., left side CS/left hand US vs. right side CS/left hand US). Spatial compatibility effects are well established in the sensory-motor domain. For example, participants respond faster when stimulus and response are compatible rather than incompatible (e.g., left side stimulus/left hand response vs. left side stimulus/right hand response), even when the stimulus position is irrelevant to the task (e.g., Cespon et al., 2020; Hommel, 2011; Simon and Small, 1969). This is thought to occur because when stimulus and response are both spatially defined (by being lateralized), response processing may prime the processing of stimulus location, thus facilitating response in compatible trials and interfering with it in incompatible trials (Hommel, 2009, 2019). A similar dynamic may be hypothesized to occur during Pavlovian conditioning, where the CS is mapped onto its somatosensory consequences (i.e., US delivery to a specific area of the body). For example, a scenario where an aversive shock is delivered onto one hand only may bias threat expectations in favor of compatible as compared to incompatible CSs. Simply put, a shock to the right hand is more likely to be caused by a visual stimulus appearing close to the right hand, than one appearing close to the left hand. Consequently, compatible CSs may be more readily associable with the US, facilitating conditioning acquisition and/or hindering its extinction.

However, a different learning dynamic may also be at play than the one just described. In fact, conditioning acts to update prior expectations to reflect current environmental contingencies (Courville et al., 2006; Mackintosh, 1975; Pearce and Hall, 1980; Rescorla and Wagner, 1972), in order to maximize survival in an ever-changing environment. In line with this, the associability of a CS to its outcome has been shown to be determined not only by the initial CS-related US expectations, but also by the actual CS' predictive power (Le Pelley, 2004). Thus, when realizing that 'surprisingly', incompatible CSs likewise represent a threat to body integrity by predicting US occurrence, prior expectations may be revised in light of current contingencies. In fact, 'surprising' events are known to produce faster learning than well predicted events (Courville et al., 2006; Le Pelley, 2004; Mackintosh, 1975; Pearce and Hall, 1980).

Following this reasoning, acquisition and/or extinction of threat conditioning may be facilitated for incompatible CSs compared to compatible ones.

On this basis, the present study investigated whether and how CS-US spatial compatibility modulates threat conditioning. We assessed whether initial expectations of threat are biased in favor of CSs appearing in a location compatible with that of the US delivery. We then tested whether and how such bias affected learning, by assessing differences in the acquisition, extinction, and recovery (following reinstatement) of threat conditioning between spatially compatible and incompatible CSs. To this end, participants completed a Pavlovian threat conditioning task while resting both hands on a computer screen horizontally placed on a table. The US was a mild aversive shock delivered to one of the participant's hands. The CSs consisted of four geometrical shapes. Crucially, two CSs always appeared in the same hemispace as the shocked hand (i.e., compatible condition), and two CSs always in the opposite hemispace (i.e., incompatible condition; Fig. 2). In addition, only one of the compatible CSs and one of the incompatible CSs was paired with the US (i.e., CS+), while the other CS from each compatibility condition was never paired with the US (i.e., CS-). To assess conditioning, skin conductance response (SCR) was recorded and used to analyze changes in mean SCR during each task phase. Additionally, we used computational modeling to characterize participants' initial expectations of CS-US associations and the rate at which these expectations are updated on a trial-by-trial basis (Atlas and Phelps, 2018; Li et al., 2011; Stussi et al., 2021). Before learning which CSs predict US occurrence, we expected an initial bias in threat expectations in favor of compatible CSs. With respect to threat conditioning, we compared the two following competing predictions. On one hand, the initial bias in threat expectations may be expected to facilitate conditioning and/or hinder extinction and/or facilitate recovery for the compatible CS+. On the other hand, as participants learn that both the incompatible and compatible CSs+ predict the US delivery at the same rate, the initial bias may be overcome or offset, with facilitated acquisition and/or extinction and recovery of threat response for the incompatible than the compatible CS+.

## 1. Methods

### 1.1. Participants

Twenty-four healthy participants were recruited from the young adult population of the town of Cesena (Italy). One participant was removed from the analysis due to computer malfunctioning, one for failing to show SCR, and two participants for failing to report the correct stimulus-outcome (i.e., CS-US) contingencies (as previously done in Starita et al., 2016). These exclusion criteria were established prior to data collection. This left a total of 20 participants in the analysis (10 males; age  $M = 22.50$  years,  $SD = 3.65$  years).

A sensitivity power analysis was performed with MorePower 6.0 (Campbell and Thompson, 2012) using the following parameters (based on the planned statistical analyses, see below): repeated measures ANOVA; sample size = 20; numerator  $df = 1$ , denominator  $df = 19$ ;  $\alpha = 0.05$ . This was used to produce a sensitivity curve (Fig. 1), which shows the power of detecting a significant effect by our statistical analyses given an a-priori range of plausible effect sizes for our paradigm (Lakens, 2022).

The study followed the American Psychological Association Ethical Principles of Psychologists and Code of Conduct and the Declaration of Helsinki, and was approved by the Bioethics Committee of the University of Bologna (Prot. 71559). All participants provided written informed consent to participation. The study was not preregistered.

### 1.2. Pavlovian threat conditioning task

Fig. 2 shows an illustration of the task. The conditioned stimuli (CSs)

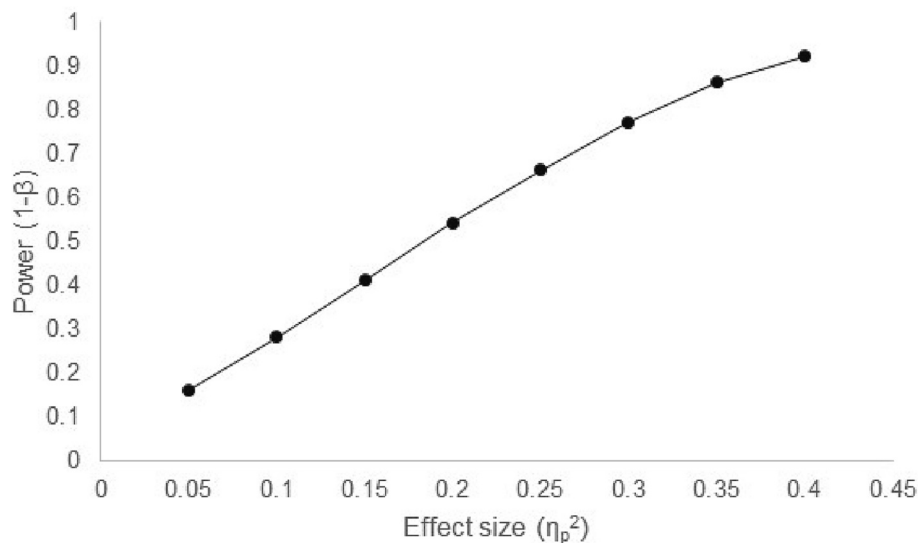


**Fig. 1.** Sensitivity curve. The plot shows the power of our statistical analyses for a range of a-priori plausible effect sizes, given a sample size of 20 participants, an alpha level of 0.05 and a RM ANOVA with (1,19) degrees of freedom.

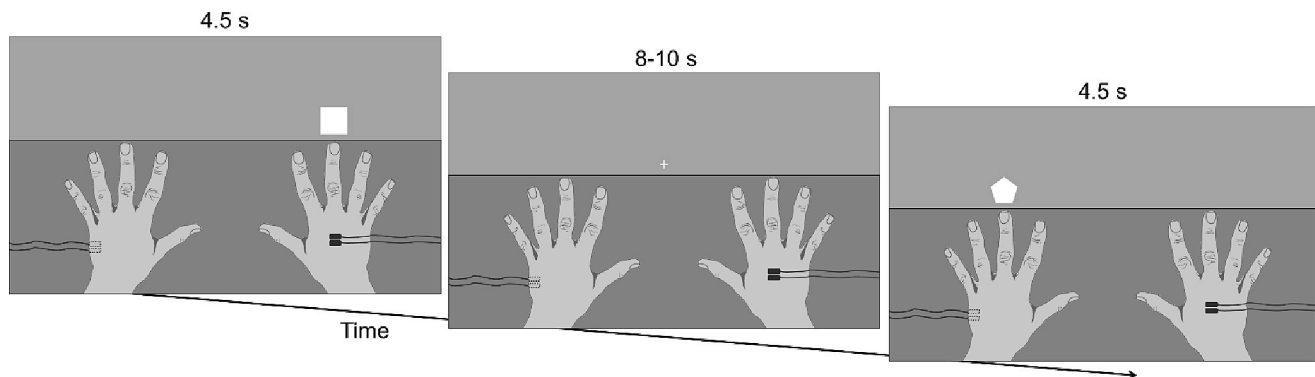


**Fig. 2.** Pavlovian threat conditioning task. The figure shows shock electrodes placed on the right hand and SCR electrodes on the left hand. Thus, the left screen represents an example of a compatible CS trial, while the right screen represents an example of an incompatible CS trial and the middle screen an example of the inter-trial interval. Only the light gray section of the screen was visible to participants, as vision of the hands was occluded by a piece of cardboard, here represented by the dark gray rectangle.

were images of four different white geometrical shapes (i.e., triangle, square, pentagon, octagon), which appeared on a gray background. Two of the CSs always appeared 32.5 cm to the left of the center of the screen and the two others always appeared 32.5 cm to the right. Additionally, on each side, one CS was the threat conditioned stimulus (CS+) and the other the within-participant control stimulus (CS-). Shape assignment to each CS role was counterbalanced between participants. The unconditioned stimulus (US) consisted of a 0.2-ms aversive electrical shock generated by a Digitimer Stimulator (Model DS7A, Digitimer Ltd., UK) and delivered to the participants' dorsal side of the left or right hand (counterbalanced between participants) through pre-gelled Ag/AgCl snapped electrodes (Friendship Medical, SEAg-S-15000/15x20). The US intensity ( $M = 22.95$  mA,  $SD = 15.03$ ) was calibrated for each participant to a level deemed "highly unpleasant, but not painful" using an ascending staircase procedure. Participants rated the unpleasantness of the shock ( $M = 7.26$ ,  $SD = 0.80$ ) on a scale ranging from 0 (*no sensation*) to 10 (*painful*).

The stimuli appeared on a 43-in. computer screen (resolution: 1920 × 1080; refresh rate: 60 Hz), at a viewing distance of ~60 cm. A PC running MATLAB controlled stimulus presentation and shock delivery. The screen on which the stimuli appeared was placed horizontally on a table and participants' hands rested on the lower portion of the screen to

the left and right of the center, right below the location of CSs appearance. Vision of the hands was occluded by a piece of cardboard, to limit the possibility that a difference in response to compatible versus incompatible CSs could be explained by a difference in visual attention posited to the shocked hand (Di Pellegrino and Frassinetti, 2000). Thus, participants saw only the portion of the screen where the stimuli appeared. These manipulations resulted in the presentation of each CS being either incompatible or compatible relative to the shocked hand (though equidistant from the participant's trunk), thus creating four within-participant experimental conditions: CS+<sub>Inc</sub>, CS+<sub>Com</sub>, CS-<sub>Inc</sub>, CS-<sub>Com</sub>. On each trial, one CS was presented for 4.5 s followed by a jittered 8–10-s intertrial interval (ITI), during which a fixation cross was presented in the center of the screen.

The task began with a habituation phase, which included 8 trials (2 trials per CS). The following acquisition phase included 64 trials (16 trials per CS). In this phase, presentation of the CS+<sub>Inc</sub> and the CS+<sub>Com</sub> co-terminated with the delivery of the US in 9 out of 16 trials (56 % reinforcement rate). Presentation of the CS-<sub>Inc</sub> and the CS-<sub>Com</sub> was never paired with the US. The subsequent extinction phase included 64 trials (16 trials per CS), during which the US was no longer delivered. Extinction was immediately followed by reinstatement, which consisted of the delivery of three consecutive unsignaled shocks between two ITIs.

The final recovery phase then occurred and included 16 unreinforced trials (4 trials per CS). Except for the first four acquisition trials that started with two CS- trials and two reinforced CS+ trials (one for each compatibility condition), in random order, trials proceeded in pseudo-random order, such that no more than two consecutive stimuli of the same type occurred in a row.

### 1.3. Procedure

Participants were comfortably seated in a silent and dimly lit room, and their position was centered relative to the computer screen. Electrodes for SCR recording and for shock delivery were attached to them. Next, their hands were placed on the screen and, after verifying correct recording of SCR, the shock intensity was calibrated. Participants were then instructed that four different shapes would appear one at the time on the screen and that two of them would always appear on the right, whereas the two others would always appear on the left. Also, they were told that some shapes might be associated with the shock, and that their task was to pay attention to the screen and try to predict which shape/s would give them the shock. Note that no information was provided regarding which stimulus would be associated with the shock, and participants had to learn the CSs-US relationship from experience. At the end of the conditioning task, participants completed subjective ratings of CS valence and arousal, and their awareness of the CS-US contingencies was tested (see dependent variables).

### 1.4. Dependent variables

#### 1.4.1. Skin conductance response (SCR)

Galvanic skin conductance was recorded at 1250 Hz, with a 10 Hz low-pass filter, from pre-gelled snap electrodes (BIOPAC EL501) placed on the hypothenar eminence of the palmar surface of the non-shocked hand, connected to a BIOPAC MP-150 System (Goleta, CA). The digitalized signal was down-sampled at 200 Hz and processed using Autonomate 2.8 (Green et al., 2014) to obtain trough-to-peak SCR values. This scoring method was chosen based on previous work from our laboratories (e.g., Starita et al., 2019, 2022, 2023; Stussi et al., 2018, 2021) and because (a) trough-to-peak SCR scoring is one of the most prevailing and validated non model-based SCR quantification approach in Pavlovian threat conditioning (e.g., Kuhn et al., 2022; Privratsky et al., 2020); and (b) the Autonomate software has been validated under similar experimental conditions to those of this study, namely 4-s CS duration and ~ 9-s average ITI duration (see Green et al., 2014, for details). Critically, results based on SCRs scored with Autonomate have been found to be comparable to those obtained with model-based scoring methods, such as implemented with SCRalyze (now called PsPM) and Ledalab (Green et al., 2014). Additionally, both non-model-based and model-based SCR quantification approaches have been shown to discriminate between CS+ and CS- without any statistically significant difference in precision and that no single approach has been demonstrated to yield consistently higher effect sizes relative to the others (Kuhn et al., 2022). A SCR was considered valid if the trough-to-peak deflection started between 0.5 and 4.5 s following the CS onset, lasted for maximum 5 s, and was  $>0.02 \mu\text{S}$ . Trials that did not meet these criteria were scored as zero and remained in the analyses (Starita et al., 2019). To standardize the data, within-participant z-scores were calculated using the mean and standard deviation of all non-reinforced trials. Reinforced trials were excluded from the z-score calculation because SCR on those trials was disrupted by the shock delivery (see Society for Psychophysiological Research Ad Hoc Committee on Electrodermal Measures, 2012).

#### 1.4.2. Subjective ratings of CSs valence and arousal

To have an explicit measure of subjective experience, participants rated how they had felt during the presentation of each CS in terms of arousal and valence on the 9-point Self-Assessment Manikin (Bradley

and Lang, 1994) presented on the PC screen, at the end of the task. Data of one participant were not collected due to software malfunctioning.

#### 1.4.3. Side of CS presentation awareness and CS-US contingency awareness

To evaluate explicit awareness of the side of presentation of each CS and explicit learning of the CS-US associations, each CS appeared on the PC screen and participants had to make a forced-choice response about the side of stimulus presentation (left/right) and whether or not (yes/no) this had been associated with the shock during the task. Data from participants who failed to answer correctly were not analyzed ( $n = 2$ ). Thus, all participants included in the analysis reported the correct associations.

### 1.5. Data analysis

#### 1.5.1. Mean SCR

Following standard practice in the human conditioning literature (see, e.g., Lonsdorf et al., 2017), each experimental phase was analyzed separately to test whether and how the CS compatibility (i.e., Compatible vs. Incompatible) from the shocked hand affected threat conditioning. The habituation phase included only the second CS trial of each condition, to minimize the effects of initial orienting responses. The acquisition phase included only unreinforced CS+ trials and all CS- trials. This phase was split into an early (i.e., mean of the first eight CS- trials, mean of the first three CS+ trials) and a late (i.e., mean of the remaining eight CS- trials, mean of the remaining four CS+ trials) block, to test for differences in the speed and/or magnitude of acquisition between the compatible and incompatible stimuli (see Stussi et al., 2018, 2021). The extinction phase included all CS trials, and was likewise split into an early (i.e., mean of the first eight CS trials for each CS) and a late (i.e., mean of the following eight CS trials for each CS) block. Finally, the recovery phase also included all CS trials, but this time, given the transient effects of reinstatement (Haaker et al., 2014), trials were not averaged but kept separate in the analysis.

#### 1.5.2. Computational modeling

We used computational modeling (see e.g. Li et al., 2011; Pearce and Hall, 1980; Rescorla and Wagner, 1972) to examine at a mechanistic level how the CS spatial compatibility affects threat conditioning. We fitted different standard reinforcement learning models to the trial-by-trial z-scored skin conductance response (SCR) data to estimate the models' free parameters and identify the best-fitting model. The candidate models included (1) the Rescorla-Wagner model (Rescorla and Wagner, 1972), (2) a modified version of the Rescorla-Wagner model with dual learning rates for excitatory and inhibitory learning (e.g., Niv et al., 2012; Stussi et al., 2018, 2021), (3) the hybrid model combining the Pearce-Hall associability mechanism with the Rescorla-Wagner model (e.g., Homan et al., 2019; Li et al., 2011; Pearce and Hall, 1980; Zhang et al., 2016) and (4) a modified version of the hybrid model incorporating dual (static) learning rates for excitatory and inhibitory learning (see Stussi et al., 2018, 2021, for a similar modeling approach). A model comparison procedure (see supplementary materials) using the Bayesian information criterion (BIC) indicated that the Rescorla-Wagner model with dual learning rates provided the best fit to the SCR data compared to the alternative models. Accordingly, we report this model in detail below as well as the results based on the learning parameters extracted from this model (for a detailed description of the alternative models considered, see supplemental materials). The dual-learning-rate Rescorla-Wagner model consists of an adaptation of the standard version of the Rescorla-Wagner model (Rescorla and Wagner, 1972) by implementing distinct learning rates for positive (i.e., when the outcome is unexpectedly delivered or more than predicted; excitatory learning) and negative (i.e., when the outcome is unexpectedly omitted or less than predicted; inhibitory learning) prediction errors (see Niv et al., 2012; Stussi et al., 2018, 2021). This model assumes that skin conductance correlates with the expected value of a CS, and that learning occurs

when there is a discrepancy between expectations and actual outcomes (i.e., a prediction error; Atlas et al., 2016; Atlas and Phelps, 2018). Excitatory and inhibitory learning rates, in turn, determine the extent to which positive and negative prediction errors are integrated in the computation of the updated CS expected value, respectively (see Niv and Schoenbaum, 2008). Formally, in the dual-learning-rate Rescorla-Wagner model, the expected value  $V$  of a given CS  $j$  is updated based on the sum of the current expected value  $V_j$  and the prediction error at trial  $t$  (i.e., the difference between  $V_j$  and the outcome  $R$  at that trial), weighted by different learning rates for positive and negative prediction errors, as follows:

$$V_j(t+1) = \begin{cases} V_j(t) + \alpha^+ \cdot (R(t) - V_j(t)) & \text{if } R(t) - V_j(t) > 0 \\ V_j(t) + \alpha^- \cdot (R(t) - V_j(t)) & \text{if } R(t) - V_j(t) < 0 \end{cases}$$

where the learning rate for positive prediction errors  $\alpha^+$  and the learning rate for negative prediction errors  $\alpha^-$  are free parameters within the range [0, 1]. If the US was delivered on the current trial  $t$ ,  $R(t) = 1$ , else  $R(t) = 0$ . To account for the fact that the various CSs may lead to differential SCR as a function of their compatibility with the threatened hand prior to conditioning, we additionally modeled the CS initial expected value ( $V_0$ ) as a free parameter ranging within [0, 1]. This model enables to capture and test how incompatible and compatible CSs can differentially modulate (a) initial responding (through the CS initial values), (b) excitatory learning (through the learning rate for positive prediction errors; e.g., during acquisition), and (c) inhibitory learning (through the learning rate for negative prediction errors; e.g., during extinction).

We modeled and extracted separate free parameters for each CS compatibility. The free parameters were estimated by fitting the model to the individual z-scored SCR data, and the trial-by-trial CS values were calculated using the best-fitting parameters for each participant. Because the model is not able to adequately produce or capture recovery effects following reinstatement, as is the case for most of the classical formal models of associative learning (see, e.g., Dunsmoor et al., 2015; Gershman et al., 2017), we omitted trials of the recovery phase from the fitting procedure. A parameter and a model recovery analysis confirmed that parameters from this model can be recovered and that the model shows virtually perfect identifiability (see supplemental materials). To test whether and how the CS compatibility with the shocked hand affects Pavlovian threat conditioning, we then proceeded by comparing the estimated initial expected values, as well as the estimated excitatory and inhibitory learning rates between the incompatible and compatible conditions.

### 1.5.3. Statistical analyses

Analyses were performed with JASP 0.14.1.0 (JASP Team, 2020) and included frequentist and Bayesian inference. Repeated-measures analyses of variance (RM ANOVA) were used to investigate differences between conditions followed by planned contrast analyses using two-tailed paired  $t$ -tests, wherever appropriate. Regarding frequentist ANOVAs, a statistical significance threshold of  $p < .05$  was adopted. Degrees-of-freedom were Greenhouse-Geisser corrected, whenever a violation of the sphericity assumption occurred. Bonferroni correction was applied to planned contrasts to correct for multiple comparisons. Partial eta-squared ( $\eta_p^2$ ) and 90 % confidence intervals (CI) were computed as estimates of effect sizes for the ANOVAs' main effects and interactions, while Cohen's  $d_z$  and 95 % CI were computed for the planned contrasts (Lakens, 2013). Regarding Bayesian ANOVAs, the Bayes Factors (BF) were generated as BF inclusion values ( $BF_{\text{incl}}$ ) quantifying the likelihood of the data under all models with a particular effect, compared to likelihood of the data under all models without that particular effect (i.e., effects across matched models), or BF exclusion values ( $BF_{\text{excl}}$ ), when  $BF_{\text{incl}} < 1$ , reflecting the likelihood of the data under all models without a particular effect, compared to all models with that particular effect. Thus, BFs of main effects compared the model with (or without) the main effect in question to the null (or alternative)

model, while BFs of interaction effects compared the model including (or excluding) the interaction term to the model including all the other terms except for (or including also) the interaction. For reproducibility, the sampling seed was set to 1. Finally, estimation plots were produced to illustrate the data (Cumming and Calin-Jageman, 2016; Ho et al., 2019).

Data and code are publicly available on <https://osf.io/cds4k/>

## 2. Results

### 2.1. Mean SCR

#### 2.1.1. Habituation

We conducted a 2 (stimulus: CS+, CS-)  $\times$  2 (compatibility: incompatible, compatible) RM ANOVA to assess differences in SCR to the CSs before any US was delivered. We observed a main effect of compatibility ( $F_{(1, 19)} = 10.59, p = .004, \eta_p^2 = 0.36, 90\% \text{ CI } [0.08, 0.55]$ ;  $BF_{\text{incl}} = 122.038$ ), showing higher SCR to compatible than incompatible CSs (Compatible:  $M = 0.81, SD = 0.92$ ; Incompatible:  $M = 0.15, SD = 0.59$ ). No other effects emerged (all  $ps \geq 0.201$ , all  $\eta_p^2s \leq 0.08$ ; all  $BF_{\text{excl}} \geq 1.786$ ). Thus, during habituation participants respond more to compatible than incompatible CSs (Fig. 3).

#### 2.1.2. Acquisition

We conducted a 2 (block: early, late)  $\times$  2 (stimulus: CS+, CS-)  $\times$  2 (compatibility: incompatible, compatible) RM ANOVA to test whether SCR was modulated by CSs compatibility with the shocked hand and CSs association (or absence thereof) with the US, as a function of block. We observed a main effect of block ( $F_{(1, 19)} = 16.85, p < .001, \eta_p^2 = 0.47, 90\% \text{ CI } [0.17, 0.63]$ ;  $BF_{\text{incl}} = 13,386.960$ ), indicating higher SCR in early than in late acquisition (Early:  $M = 0.35, SD = 0.45$ ; Late:  $M = -0.80, SD = 0.27$ ). The frequentist ANOVA additionally showed a main effect of compatibility ( $F_{(1, 19)} = 4.84, p = .040, \eta_p^2 = 0.20, 90\% \text{ CI } [0.005, 0.42]$ ), reflecting higher SCR to the compatible than the incompatible CSs (Compatible:  $M = 0.20, SD = 0.32$ ; Incompatible:  $M = 0.07, SD = 0.32$ ), but this main effect was not supported by Bayesian analysis ( $BF_{\text{excl}} = 1.791$ ). Crucially, there was also a main effect of stimulus ( $F_{(1, 19)} = 13.93, p = .001, \eta_p^2 = 0.42, 90\% \text{ CI } [0.13, 0.60]$ ;  $BF_{\text{incl}} = 1.076 \times 10^6$ ), indicating higher SCR to the CSs+ than the CSs- (CSs+:  $M = 0.39, SD = 0.58$ ; CSs-:  $M = -0.12, SD = 0.14$ ). No interaction effect was found (all  $p \geq .097$ , all  $\eta_p^2s \leq 0.14$ ; all  $BF_{\text{excl}} \geq 2.479$ ). In particular, the CS by compatibility interaction was not statistically significant ( $F(1, 19) = 0.15, p = .700, \eta_p^2 = 0.01, 90\% \text{ CI } [0.00, 0.15]$ ). A Bayesian ANOVA indicated that the data was about four times more likely under a model excluding this interaction than under a model including it ( $BF_{\text{excl}} = 4.350$ ). Similarly, the block by stimulus by compatibility interaction was not statistically significant ( $F(1, 19) = 0.68, p = .420, \eta_p^2 = 0.04, 90\% \text{ CI } [0.00, 0.21]$ ) and the data was about twice more likely under the model excluding this term than under the model including it ( $BF_{\text{excl}} = 2.619$ ). Thus, during acquisition, SCR appeared to decrease from early to late trials, an effect not uncommon for such measure (Lonsdorf et al., 2017; see also e.g., Battaglia et al., 2018; Starita et al., 2016). Crucially, participants showed successful threat conditioning, responding more to the CSs+ than the CSs-, to a comparable degree between compatible and incompatible CSs. Converging evidence for this is also found in estimation statistics shown in the lower plot of Fig. 4. As can be observed, the 95 % confidence intervals of the differential SCRs represented in the lower plot are greater than zero and of comparable magnitude (due to the overlap of confidence intervals) across compatibility conditions and blocks.

#### 2.1.3. Extinction

We conducted a 2 (block: early, late)  $\times$  2 (stimulus: CS+, CS-)  $\times$  2 (compatibility: incompatible, compatible) RM ANOVA to test whether SCR to the CSs was modulated by CSs compatibility with the shocked hand and CS previous association (or lack thereof) with the US, as a

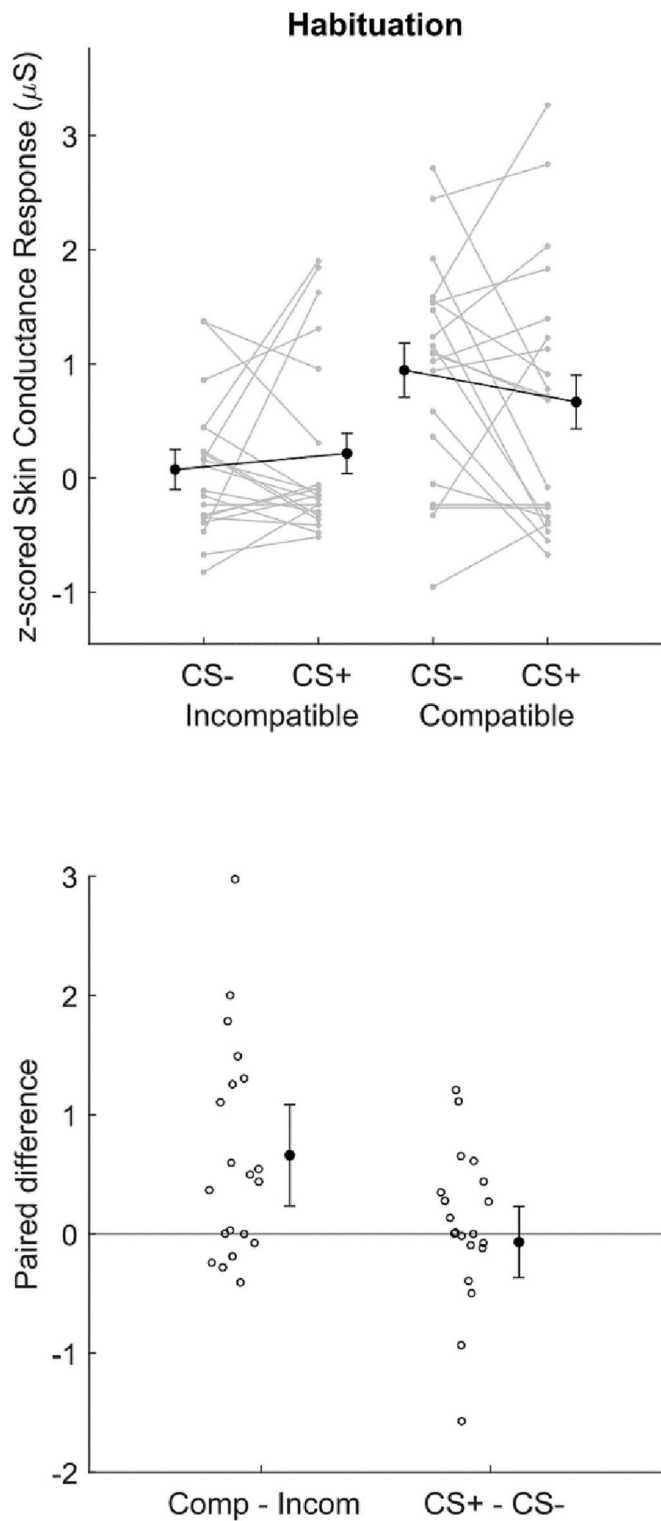


Fig. 3. Habituation. The upper plot shows individual participants' data (gray dots), group means (black dots) and 95 % confidence intervals (vertical black lines) of z-scored SCR to CS+ and CS- as a function of compatibility. Each paired set of observations is connected by a gray line, confidence intervals were corrected for within-subjects design (Cousineau, 2005). The lower plot shows individual participants' paired difference (white dots), group paired mean differences (black dots) and 95 % confidence intervals (vertical black lines) between z-scored SCR to incompatible and compatible trials, and CS+ and CS-. Confidence intervals of paired mean differences were calculated with the ESCI module for Jamovi (Cumming and Calin-Jageman, 2016).

function of block. We observed a main effect of stimulus ( $F_{(1, 19)} = 9.87, p = .005, \eta_p^2 = 0.34, 90\% \text{ CI } [0.07, 0.54]; \text{BF}_{\text{incl}} = 2.262 \times 10^4$ ), and a block-by-stimulus interaction ( $F_{(1, 19)} = 7.90, p = .011, \eta_p^2 = 0.29, 90\% \text{ CI } [0.08, 0.55]; \text{BF}_{\text{incl}} = 6.701$ ). Crucially, these effects were qualified by the block-by-stimulus-by-compatibility interaction ( $F_{(1, 19)} = 7.68, p = .012, \eta_p^2 = 0.29, 90\% \text{ CI } [0.04, 0.50]; \text{BF}_{\text{incl}} = 2.310$ ). Follow-up two-tailed paired *t*-tests (Bonferroni corrected critical *p* value = .0125) showed greater SCR to the incompatible CS+ than CS- in early trials, but not in late trials (Early: CS+:  $M = 0.27, SD = 0.64$ ; CS-:  $M = -0.43, SD = 0.20$ ;  $t(19) = 4.23, p < .001$ , Cohen's  $d_z = 0.95, 95\% \text{ CI } [0.41, 1.47]; \text{BF}_{10} = 73.05$ ; Late: CS+:  $M = -0.21, SD = 0.34$ ; CS-:  $M = -0.29, SD = 0.36$ ;  $t(19) = 0.66, p = .52$ , Cohen's  $d_z = 0.15, 95\% \text{ CI } [-0.29, 0.59]; \text{BF}_{10} = 0.28$ ). In contrast, for compatible stimuli, SCR was also greater to CS+ than CS- in early trials, although this difference did not survive correction for multiple comparisons and Bayesian analyses showed only weak evidence for it (CS+:  $M = 0.01, SD = 0.54$ ; CS-:  $M = -0.32, SD = 0.2030$ ;  $t(19) = 2.17, p = .043$ , Cohen's  $d_z = 0.48, 95\% \text{ CI } [0.01, 0.94]; \text{BF}_{10} = 1.56$ ). Additionally, in late trials, the frequentist *t*-test showed no statistically significant difference in SCR between the compatible CS+ and the CS-, while the Bayesian *t*-test showed only weak evidence for such difference (CS+:  $M = -0.11, SD = 0.36$ ; CS-:  $M = -0.35, SD = 0.31$ ;  $t(19) = 1.99, p = .06$ , Cohen's  $d_z = 0.44, 95\% \text{ CI } [-0.02, 0.90]; \text{BF}_{10} = 1.18$ ). Finally, two-tailed paired *t*-tests showed greater conditioned response (i.e., CS+ - CS-) to incompatible than compatible stimuli in early but not late extinction (Early: Incompatible:  $M = 0.70, SD = 0.74$ , Compatible:  $M = 0.33, SD = 0.68$ ;  $t(19) = 2.54, p = .020$ , Cohen's  $d_z = 0.57, 95\% \text{ CI } [0.09, 1.04]; \text{BF}_{10} = 2.91$ ; Late: Incompatible:  $M = 0.08, SD = 0.51$ , Compatible:  $M = 0.25, SD = 0.55$ ;  $t(19) = -1.50, p = .149$ , Cohen's  $d_z = -0.34, 95\% \text{ CI } [-0.78, 0.12]; \text{BF}_{10} = 0.61$ ). Thus, at the beginning of extinction, the conditioned response was greater to incompatible than compatible CSs, but it was extinguished for both incompatible and compatible CSs by the end of extinction (Fig. 5).

#### 2.1.4. Recovery following reinstatement

We conducted a 2 (stimulus: CS+, CS-)  $\times$  2 (compatibility: incompatible, compatible)  $\times$  4 (trials: 1–4) RM ANOVA to examine differences in SCR to the CSs as a function of their compatibility with the shocked hand and their previous association (or lack thereof) with the US after threat reinstatement. We observed a main effect of trial ( $F_{(1, 47, 27.91)} = 15.47, p < .001, \eta_p^2 = 0.45, 90\% \text{ CI } [0.26, 0.55]; \text{BF}_{\text{incl}} = 2.183 \times 10^{11}$ ) and a compatibility-by-stimulus interaction ( $F_{(1, 57)} = 5.09, p = .036, \eta_p^2 = 0.21, 90\% \text{ CI } [0.01, 0.24]; \text{BF}_{\text{incl}} = 1.781$ ). However, these effects were qualified by a compatibility-by-stimulus-by-trial interaction ( $F_{(1, 82, 43.59)} = 5.13, p = .013, \eta_p^2 = 0.21, 90\% \text{ CI } [0.051, 0.33]; \text{BF}_{\text{incl}} = 2.421$ ). In the incompatible condition, follow-up two-tailed paired *t*-tests (Bonferroni corrected critical *p* value = .0062) indicated greater SCR to the CS+ than the CS- in the first trial (CS + Inc:  $M = 2.00, SD = 2.07$ ; CS- Inc:  $M = 0.70, SD = 1.66$ ;  $t(19) = 3.10, p = .006$ , Cohen's  $d_z = 0.69, 95\% \text{ CI } [0.19, 1.17]; \text{BF}_{10} = 7.919$ ), but not in other trials (all *ps*  $\geq 0.189$ , all  $\text{BF}_{s10} \leq 0.525$ ). In contrast, in the compatible condition, there was no difference in SCR between the CS+ and the CS- in any of the recovery trials (all *ps*  $\geq 0.010$ ; all  $\text{BF}_{s10} \leq 0.383$ ). Thus, in the first trial of recovery following reinstatement, the conditioned response was recovered to incompatible but not compatible CSs (Fig. 6).

## 2.2. Computational modeling

### 2.2.1. Estimated initial expected values

We conducted a two-tailed paired *t*-test to assess differences in estimated CS initial expected values as a function of CS compatibility with the shocked hand. Results showed greater initial expected value for compatible than incompatible CSs, although this difference did not reach statistical significance (Incompatible:  $M = 0.44, SD = 0.23$ ; Compatible:  $M = 0.57, SD = 0.25$ ;  $t(19) = 1.75, p = .095$ , Cohen's  $d_z = 0.39, 95\% \text{ CI } [-0.07, 0.48,]; \text{BF}_{10} = 0.847$ ; Fig. 7).

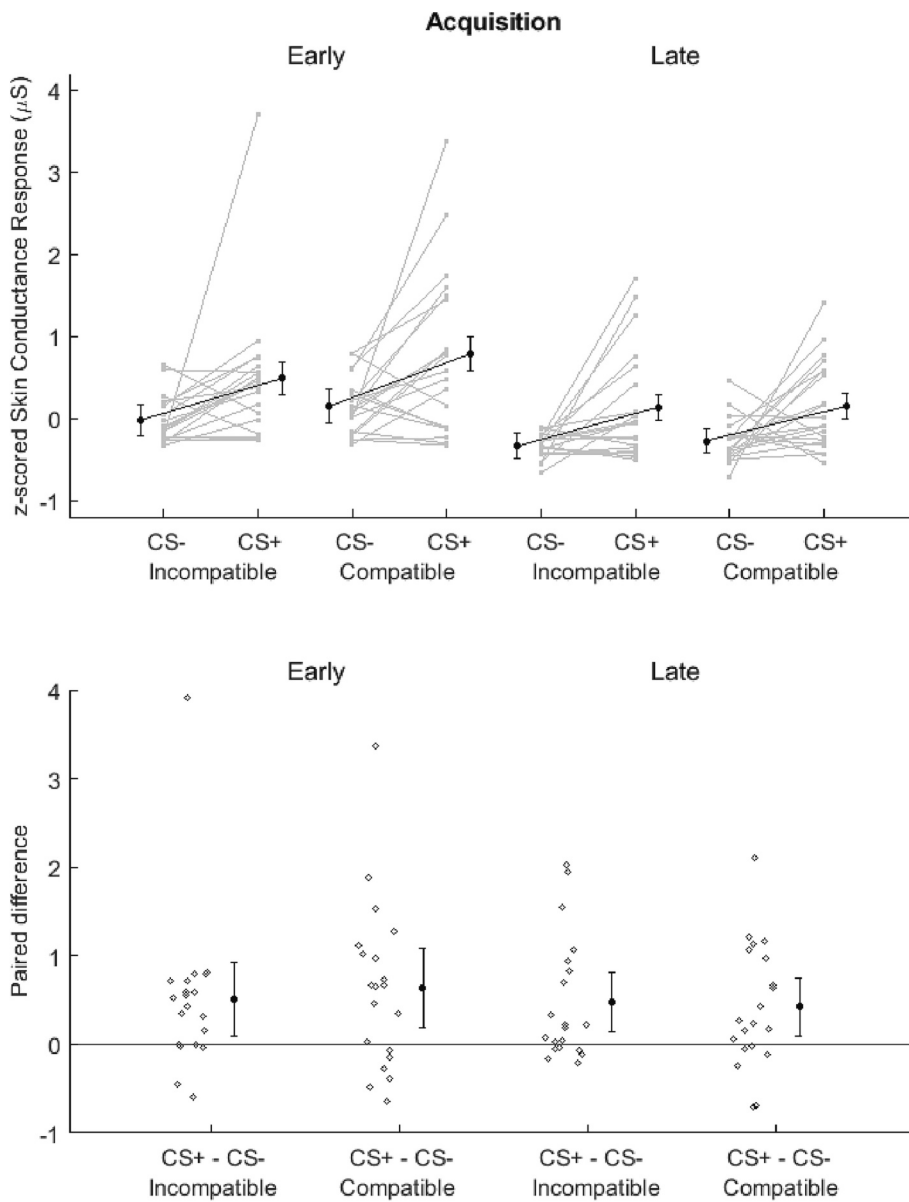


**Fig. 4.** Acquisition. The upper plot shows individual participants' data (gray dots), group means (black dots) and 95 % confidence intervals (vertical black lines) of z-scored SCR to CS+ and CS- as a function of compatibility and block. Each paired set of observations is connected by a gray line, confidence intervals were corrected for within-subjects design (Cousineau, 2005). The lower plot shows individual participants' paired difference (white dots), group paired mean differences (black dots) and 95 % confidence intervals (vertical black lines) between z-scored SCR to CS+ and CS- as a function of compatibility and block. Confidence intervals of paired mean differences were calculated with the ESCI module for Jamovi (Cumming and Calin-Jageman, 2016).

2.2.2. Estimated learning rates

We conducted two separate two-tailed paired *t*-test to assess differences in learning-rates estimates as a function of CS compatibility with the shocked hand, separately for excitatory and inhibitory learning rates. The results on excitatory learning rate showed a higher learning rate for the incompatible than the compatible CSs (Incompatible:  $M = 0.10, SD = 0.10$ ; Compatible:  $M = 0.07, SD = 0.08$ ;  $t_{(19)} = 2.56, p = .019$ , Cohen's  $d_z = 0.57$ , 95 % CI [0.09, 1.04];  $BF_{10} = 3.025$ ). In contrast, the results on inhibitory learning rates showed no statistically significant difference between the compatible and incompatible CSs (Incompatible:  $M = 0.40, SD = 0.34$ ; Compatible:  $M = 0.35, SD = 0.26$ ;  $t_{(19)} = 0.87, p = .40$ , Cohen's  $d_z = 0.19$ , 95 % CI [-0.25, 0.63];  $BF_{10} = 0.324$ ; Fig. 8).

2.3. Subjective ratings

2.3.1. Valence

We conducted a 2 (stimulus: CS+, CS-) × 2 (compatibility: incompatible, compatible) RM ANOVA on valence ratings to assess differences in subjective ratings among CSs. Results showed only a main effect of stimulus ( $F(1, 18) = 75.35, p < .001, \eta_p^2 = 0.81, 90\% \text{ CI } [0.62, 0.87]$ ;

$BF_{incl} = 4.920 \times 10^{17}$ ). Participants reported lower pleasantness to the CS+ than the CS- (CS+:  $M = 2.58, SD = 1.24$ ; CS-:  $M = 6.45, SD = 1.38$ ). No other effect was found (all  $ps \geq 0.207$ ; all  $BF_{s_{10}} \leq 0.265$ ).

2.3.2. Arousal

We conducted a 2 (stimulus: CS+, CS-) × 2 (compatibility: incompatible, compatible) RM ANOVA on arousal ratings to assess differences in subjective ratings among CSs. Results showed only a main effect of stimulus ( $F(1, 18) = 146.09, p < .001, \eta_p^2 = 0.89, 90\% \text{ CI } [0.77, 0.92]$ ;  $BF_{incl} = 6.343 \times 10^{23}$ ). Participants reported greater arousal to the CS+ than the CS- (CS+:  $M = 7.10, SD = 0.91$ ; CS-:  $M = 2.79, SD = 1.44$ ). No other effect was found (all  $ps \geq 0.725$ ; all  $BF_{s_{10}} \leq 0.229$ ).

3. Discussion

We investigated whether and how CS-US spatial compatibility modulated the acquisition, extinction and recovery (following reinstatement) of Pavlovian threat conditioning. Participants completed a threat conditioning task in which visual CSs appeared on the same (i.e., compatible) or opposite (i.e., incompatible) hemisphere as that of US

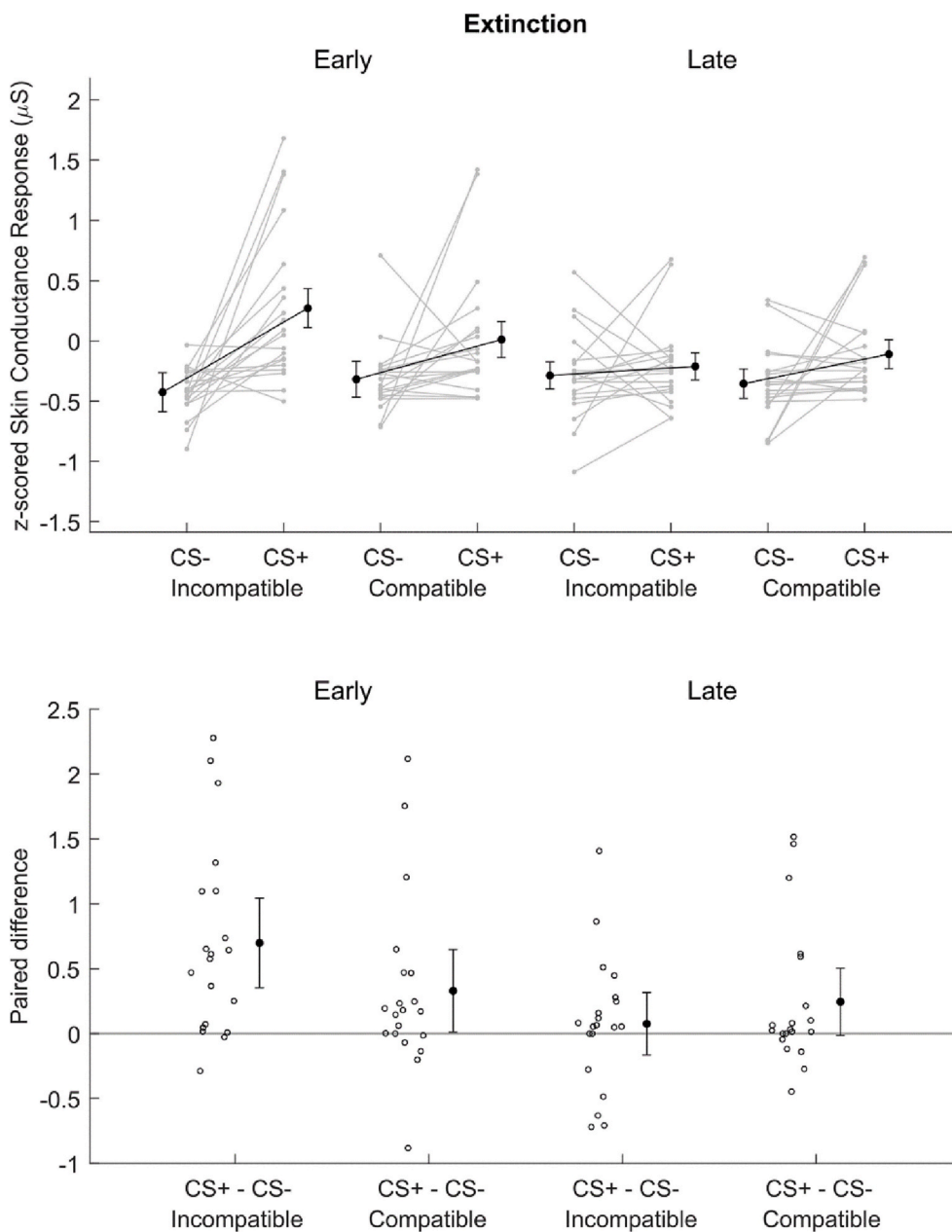


**Fig. 5.** Extinction. The upper plot shows individual participants' data (gray dots), group means (black dots) and 95 % confidence intervals (vertical black lines) of z-scored SCR to CS+ and CS- as a function of compatibility and block. Each paired set of observations is connected by a gray line, confidence intervals were corrected for within-subjects design (Cousineau, 2005). The lower plot shows individual participants' paired difference (white dots), group paired mean differences (black dots) and 95 % confidence intervals (vertical black lines) between z-scored SCR to CS+ and CS- as a function of compatibility and block. Confidence intervals of paired mean differences were calculated with the ESCI module for Jamovi (Cumming and Calin-Jageman, 2016).

delivery, consisting of an aversive shock to one hand. Results showed that, before learning which CSs predicted the shock, compatible CSs elicited greater mean skin conductance response (SCR) than incompatible ones. In contrast, during threat acquisition, when participants learned that incompatible as well as compatible CSs predicted shock delivery, SCR increased to CSs+ as compared to CSs-, indicating that the conditioned response was successfully acquired regardless of CS compatibility. Additionally, at the beginning of extinction, the conditioned response was greater to incompatible than compatible CSs (i.e., differential SCR incompatible > compatible), but it was extinguished for both incompatible and compatible CSs by the end of extinction. Similarly, following reinstatement, the conditioned response was recovered for incompatible stimuli, but rapidly re-extinguished. Finally, computational modeling analyses showed that higher SCR to compatible CSs during habituation were mirrored by a greater initial expected value in comparison to incompatible stimuli, although we note that this difference was not statistically significant. Conversely, incompatible stimuli were associated with a higher excitatory learning rate relative to

compatible stimuli, indicating that incompatible CSs induced heightened excitatory learning contributing to threat acquisition. These results suggest that stimulus-outcome spatial compatibility influences the acquisition, extinction and recovery (following reinstatement) of Pavlovian threat conditioning.

Before learning the actual source of threat (during habituation), higher mean SCR to compatible CSs suggested that threat expectations were biased in favor of stimuli whose location was compatible with the aversive outcome. Indeed, in everyday life, correspondence in spatial compatibility between a somatosensory sensation and the stimulus that caused it occurs the majority of times. Thus, at the beginning of the task, participants came into the experiment with a set of expectations, likely shaped by their long-term past experience, expecting compatible stimuli to be the source of danger. However, their initial bias was then revised during threat acquisition.

When learning that also the incompatible CS+ was a threat to body integrity during acquisition, prior expectations were revised to reflect current environmental contingencies. Thus, learning was actively



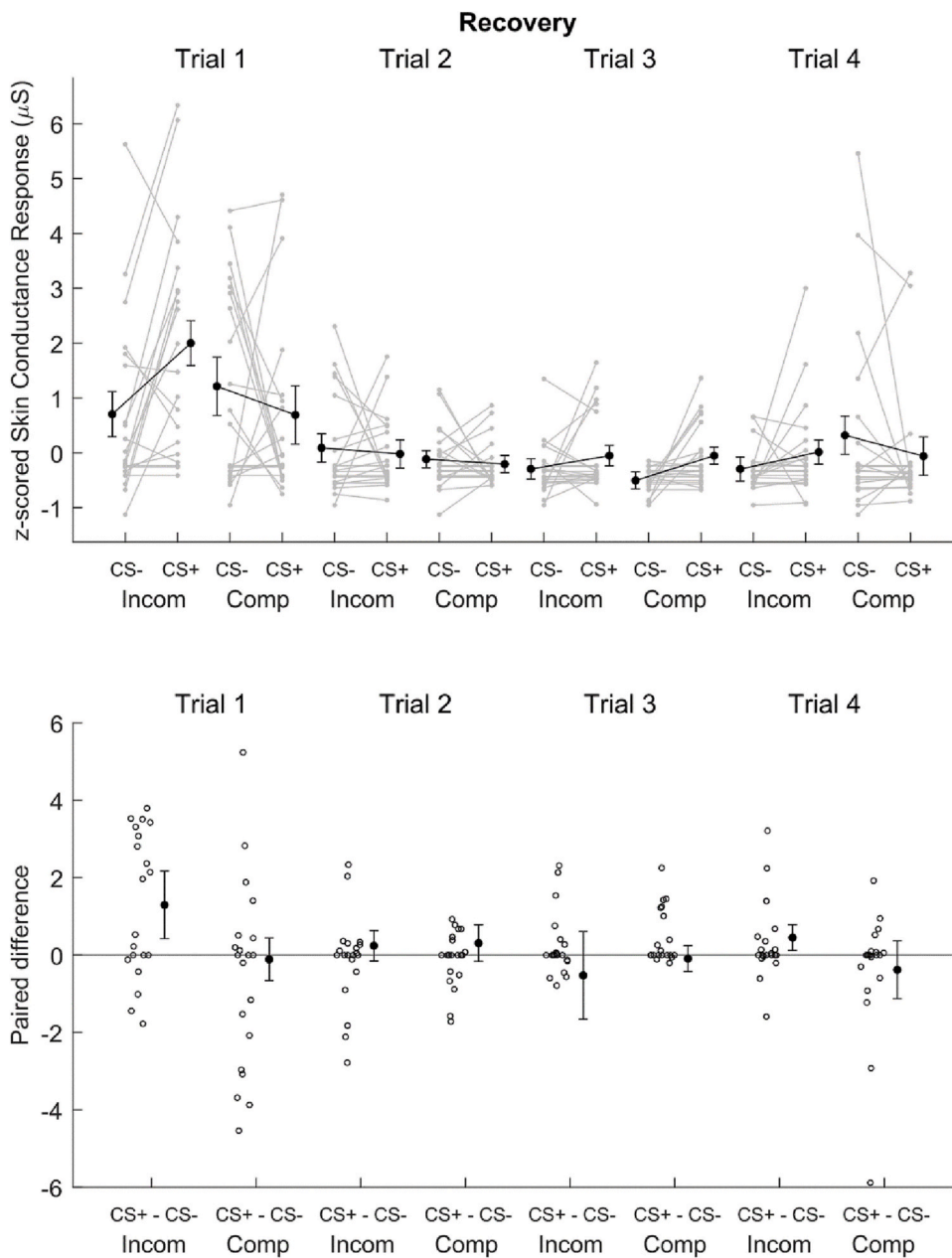


**Fig. 6.** Recovery. The upper plot shows individual participants' data (gray dots), group means (black dots) and 95 % confidence intervals (vertical black lines) of z-scored SCR to CS+ and CS- as a function of compatibility and number of trial. Each paired set of observations is connected by a gray line, confidence intervals were corrected for within-subjects design (Cousineau, 2005). The lower plot shows individual participants' paired difference (white dots), group paired mean differences (black dots) and 95 % confidence intervals (vertical black lines) between z-scored SCR to CS+ and CS- as a function of compatibility and trial number. Confidence intervals of paired mean differences were calculated with the ESCI module for Jamovi (Cumming and Calin-Jageman, 2016).

shaped by the current CS-US contingencies and not a passive reflection of initial expectations, since threat acquisition was not facilitated for compatible CS+. Although we did not observe any difference in skin conductance between compatible and incompatible stimuli during acquisition using conventional summary statistics, the higher excitatory learning rate for incompatible stimuli observed at the computational level indicated that these stimuli were associated with an enhanced update in threat expectations. Indeed, such increased excitatory learning rate resulted in weighting prediction errors following unexpected shock delivery (i.e., positive prediction errors) more for incompatible than compatible stimuli, thus having a greater impact on the update of their expected values. In other words, participants weighed more heavily the 'surprisingness' of the US for incompatible than compatible stimuli. This contributed to enhancing excitatory learning for incompatible stimuli enabling them to enter more efficiently into association with the US during acquisition. This increased excitatory learning rate may represent a mechanism whereby the initial threat expectancy bias toward compatible stimuli was offset by the facilitation of conditioned threat

acquisition for incompatible stimuli. Such mechanism enabled them to enter into association with the aversive outcome, in order to protect the body also from such less expected source of threat.

During early extinction, the higher conditioned response to incompatible stimuli relative to compatible ones suggests that extinction learning may have been slower in the first trials in response to incompatible stimuli. However, the difference in response between compatible and incompatible stimuli was no longer evident during late extinction, possibly suggesting a steeper decay in conditioned response for incompatible stimuli as extinction progressed. Nevertheless, this extinction dynamic was not reflected at the level of the inhibitory learning rates, which did not statistically differ between compatible and incompatible stimuli. A potential explanation for this discrepancy may be that inhibitory learning encompasses all trials where a negative prediction error is generated (i.e., CS+ extinction trials, but also CS+ non-reinforced acquisition trials, and all CS- trials), and therefore does not exclusively reflect extinction learning. Alternatively, it is also possible that the difference in conditioned response between incompatible and

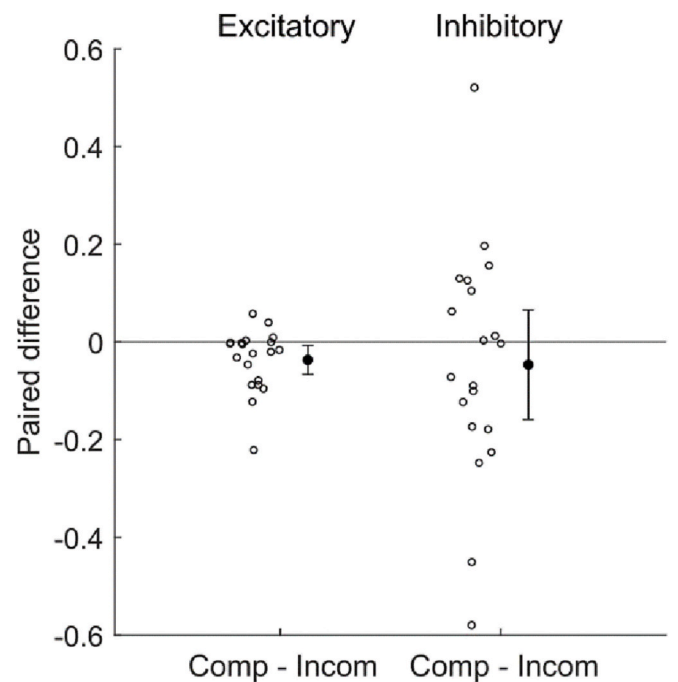
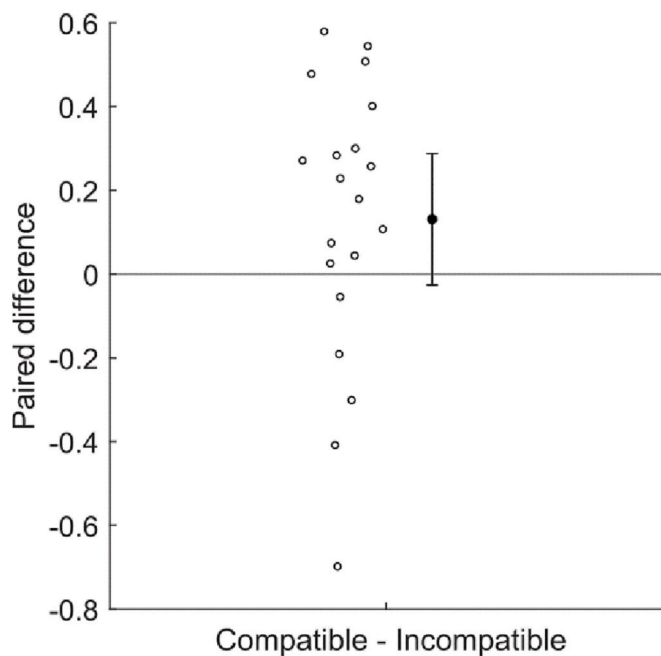
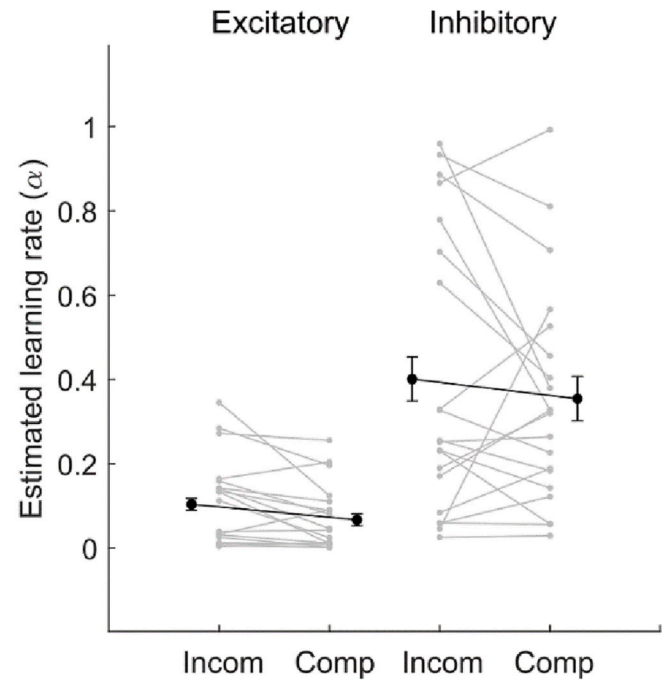
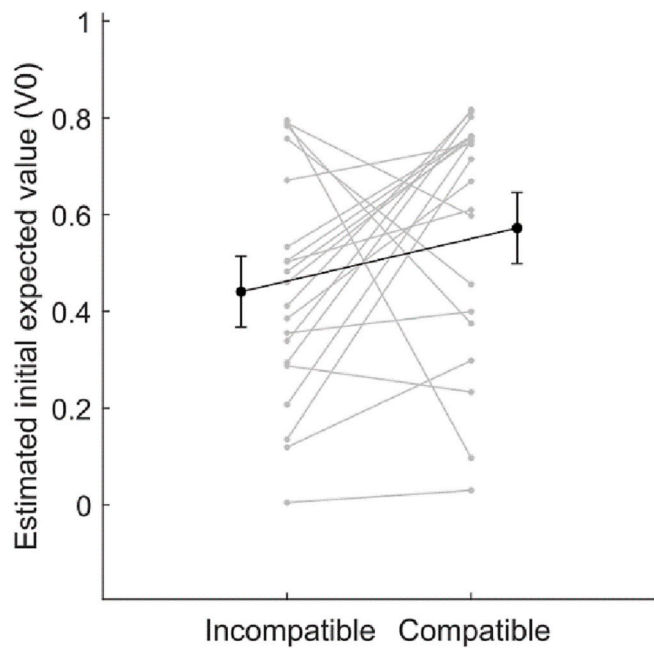


**Fig. 7.** Estimated initial expected values ( $V_0$ ). The upper plot shows individual participants' data (gray dots), group means (black dots) and 95 % confidence intervals (vertical black lines) of estimated initial expected values ( $V_0$ ) to compatible and incompatible trials. Each paired set of observations is connected by a gray line, confidence intervals were corrected for within-subjects design (Cousineau, 2005). The lower plot shows individual participants' paired difference (white dots), group paired mean differences (black dots) and 95 % confidence intervals (vertical black lines) between estimated initial expected values ( $V_0$ ) to compatible and incompatible trials. Confidence intervals of paired mean differences were calculated with the ESCI module for Jamovi (Cumming and Calin-Jageman, 2016).

**Fig. 8.** Estimated learning rates ( $\alpha$ ). The upper plot shows individual participants' data (gray dots), group means (black dots) and 95 % confidence intervals (vertical black lines) of estimated excitatory and inhibitory learning rates ( $\alpha$ ) to compatible and incompatible trials. Each paired set of observations is connected by a gray line, confidence intervals were corrected for within-subjects design (Cousineau, 2005). The lower plot shows individual participants' paired difference (white dots), group mean differences (black dots) and 95 % confidence intervals (vertical black lines) between estimated excitatory and inhibitory learning rates ( $\alpha$ ) to compatible and incompatible trials. Confidence intervals of paired mean differences were calculated with the ESCI module for Jamovi (Cumming and Calin-Jageman, 2016).

compatible stimuli during early extinction may reflect “residual” effects of the heightened excitatory learning associated with incompatible stimuli, rather than – or in addition to – differences in extinction learning per se.

Finally, during the recovery phase following reinstatement, the recovery of the conditioned response for incompatible but not compatible stimuli corroborates the idea that learning acted to revise initial threat expectations. Speculatively, such results may have been driven by the heightened excitatory learning rate to incompatible stimuli relative to compatible ones. Indeed, reinstatement likely contributed to reactivating the threat acquisition memory, which may have led to a greater return of threat to incompatible stimuli as they were associated with a higher excitatory learning rate and tentatively a putative stronger threat memory acquisition.

When related back to the literature on threat conditioning and spatial information, our results do not provide evidence that the CS that was closer to the aversive outcome (i.e., compatible) – as manipulated through spatial compatibility under our experimental conditions, with all CSs at the same distance from and in close proximity with the body – facilitate learning. Conversely, we observed a higher excitatory learning rate associated with the CS that was farther away from the US (i.e., incompatible) as well as a higher conditioned response to this stimulus during the first part of extinction and recovery. These findings appear at odds with the notion that CSs closer to the US should facilitate learning (Nasser and Delamater, 2016) and contrast with the evidence that CSs closer to the US – in terms of proximity to the body – are associated with enhanced threat acquisition and resistance to extinction (Faul et al., 2020). However, our study partially aligns with the findings of a facilitated acquisition of threat conditioning in response to CSs that are farther away from the US – by being farther away from the body (Rosén et al., 2017, 2019). In fact, if there is no difference in the threat posed by closer and farther CSs+, given the equal reinforcement rate, an adaptive strategy may be to update threat expectations more strongly to farther stimuli (initially associated with lower threat expectations), in order to appropriately defend the body from both sources of threat. Altogether, these considerations suggest that a closer CS-US spatial relationship does not always facilitate Pavlovian threat conditioning as is typically the case with the temporal relationship (e.g., Mackintosh, 1974), but that these effects might be more flexible and depend on the specific relative location of the threat cue and its associated aversive outcome.

Importantly, at variance with previous studies on spatial information (e.g., Åhs et al., 2015; Faul et al., 2020; Rosén et al., 2017, 2019), we kept all CSs at the same distance from – and in close proximity with – the body, within the so-called boundaries of peripersonal space representation (Serino et al., 2015). In such scenario, our results may suggest that the spatial relationship between the stimuli and the threatened body part appears to drive the initial arousal response (as measured with skin conductance) to those stimuli, rather than the relationship between the stimuli and the whole body. Thus, when the threat-signaling cues are in close proximity to the body, stimulus-outcome spatial relationship may be coded in a body-part frame of reference, rather than in a whole-body frame of reference. Indeed, during habituation, under maximal uncertainty regarding the actual source of threat, SCR was modulated by the CS distance from the threatened body part, with closer (i.e. compatible) stimuli eliciting greater response than farther (i.e. incompatible) ones. Importantly, the spatial relationship with the threatened body part also modulated the acquisition, extinction, and recovery of conditioned response. Thus, threat conditioning itself appears sensitive not only to the relationship between threat signaling cues and the body, as previously shown (e.g., Åhs et al., 2015; Faul et al., 2020; Rosén et al., 2017, 2019), but also to their relationship with the threatened body part. Whether the body-part reference frame is maintained even when the location of compatible and incompatible CSs is close to the body but at different distances from the US location should be evaluated in future studies (as done in the sensory-motor domain by Aglioti and Tomaiuolo, 2000, for instance), to further clarify the role of CS-US spatial distance

beyond compatibility.

The current findings should nonetheless be put into perspective to some extent, given the relatively small sample size, which is a limitation of the study. Although we performed a sensitivity power analysis to illustrate the effect sizes that could be detected with varying degrees of power given the current sample size, larger samples may be necessary to estimate more precisely the effects of stimulus-outcome compatibility on threat conditioning. Further studies with large samples might thus be warranted to provide more conclusive and robust evidence regarding the role of spatial compatibility in human Pavlovian learning.

In conclusion, the present study shows that stimulus-outcome spatial relationship influences initial threat expectations, as well as the acquisition, extinction, and recovery (following reinstatement) of Pavlovian threat conditioning. Specifically, although initial threat expectations were biased in favor of compatible stimuli, a higher excitatory learning rate was found for incompatible stimuli, indicating enhanced updating in threat expectations for the latter during the task. Additionally, we observed higher conditioned response to incompatible stimuli during early extinction and its recovery following reinstatement. These results suggest that learning may not be a passive reflection of initial expectations, but, rather, it may act to revise initial threat expectations to reflect current environmental contingencies and maximize survival. Overall, our findings contribute to the understanding of the role of spatial information in Pavlovian learning and highlight its flexible and adaptive nature.

#### Data availability

Data and code related to the manuscript are publicly available on <https://osf.io/cds4k/>

#### Appendix A. Supplementary material

Supplementary material to this article can be found online at <https://doi.org/10.1016/j.ijpsycho.2023.06.003>.

#### References

- Aglioti, S., Tomaiuolo, F., 2000. Spatial stimulus-response compatibility and coding of tactile motor events: influence of distance between stimulated and responding body parts, spatial complexity of the task and sex of subject. *Percept. Mot. Skills* 91 (1), 3–14. <https://doi.org/10.2466/pms.2000.91.1.3>.
- Åhs, F., Dunsmoor, J.E., Zielinski, D., LaBar, K.S., 2015. Spatial proximity amplifies valence in emotional memory and defensive approach-avoidance. *Neuropsychologia* 70, 476–485. <https://doi.org/10.1016/j.neuropsychologia.2014.12.018>.
- Atlas, L.Y., Phelps, E.A., 2018. Prepared stimuli enhance aversive learning without weakening the impact of verbal instructions. *Learn. Mem.* 25 (2), 100–104. <https://doi.org/10.1101/lm.046359.117>.
- Atlas, L.Y., Doll, B.B., Li, J., Daw, N.D., Phelps, E.A., 2016. Instructed knowledge shapes feedback-driven aversive learning in striatum and orbitofrontal cortex, but not the amygdala. *ELife* 5 (MAY2016). <https://doi.org/10.7554/eLife.15192>.
- Battaglia, S., Garofalo, S., di Pellegrino, G., 2018. Context-dependent extinction of threat memories: influences of healthy aging. *Sci. Rep.* 8 (1), 12592. <https://doi.org/10.1038/s41598-018-31000-9>.
- Bouton, M.E., 2007. *Learning and behavior: a contemporary synthesis*. In: *Learning and Behavior: A Contemporary Synthesis*.
- Bradley, M.M., Lang, P.J., 1994. Measuring emotion: the self-assessment manikin and the semantic differential. *J. Behav. Ther. Exp. Psychiatry*. [https://doi.org/10.1016/0005-7916\(94\)90063-9](https://doi.org/10.1016/0005-7916(94)90063-9).
- Campbell, J.I.D.D., Thompson, V.A., 2012. MorePower 6.0 for ANOVA with relational confidence intervals and Bayesian analysis. *Behav. Res. Methods* 44 (4), 1255–1265. <https://doi.org/10.3758/s13428-012-0186-0>.
- Cespón, J., Hommel, B., Korsch, M., Galashan, D., 2020. The neurocognitive underpinnings of the Simon effect: An integrative review of current research. In: *Cognitive, Affective and Behavioral Neuroscience*, Vol. 20, Issue 6. Springer, pp. 1133–1172. <https://doi.org/10.3758/s13415-020-00836-y>.
- Christie, J., 1996. Spatial contiguity facilitates Pavlovian conditioning. *Psychon. Bull. Rev.* 3, Issue 3.
- Courville, A.C., Daw, N.D., Touretzky, D.S., 2006. Bayesian theories of conditioning in a changing world. *Trends Cogn. Sci.* 10 (7), 294–300. <https://doi.org/10.1016/j.tics.2006.05.004>.
- Cousineau, D., 2005. Confidence intervals in within-subject designs: a simpler solution to Loftus and Masson’s method. In: *Tutorials in Quantitative Methods for Psychology*, 1 (1), pp. 42–45. <https://doi.org/10.20982/tqmp.01.1.p042>.

- Cumming, G., Calin-Jageman, R., 2016. Introduction to the New Statistics. In: Introduction to the New Statistics. Routledge. <https://doi.org/10.4324/9781315708607>.
- Delamater, A.R., 2012. On the nature of CS and US representations in Pavlovian learning. *Learn. Behav.* 40 (1), 1–23. <https://doi.org/10.3758/s13420-011-0036-4>.
- Di Pellegrino, G., Prassinetti, F., 2000. Direct evidence from parietal extinction of enhancement of visual attention near a visible hand. *Curr. Biol.* 10 (22), 1475–1477. [https://doi.org/10.1016/S0960-9822\(00\)00809-5](https://doi.org/10.1016/S0960-9822(00)00809-5).
- Dunsmoor, J.E., Niv, Y., Daw, N., Phelps, E.A., 2015. Rethinking extinction. *Neuron* 88 (1), 47–63. <https://doi.org/10.1016/j.neuron.2015.09.028>.
- Faul, L., Stjepanovic, D., Stivers, J.M., Stewart, G.W., Graner, J.L., Morey, R.A., LaBar, K.S., 2020. Proximal threats promote enhanced acquisition and persistence of reactive fear-learning circuits. *Proc. Natl. Acad. Sci. U. S. A.* 117 (28), 16678–16689. <https://doi.org/10.1073/pnas.2004258117>.
- Gershman, S.J., Monfils, M.H., Norman, K.A., Niv, Y., 2017. The computational nature of memory modification. *eLife* 6. <https://doi.org/10.7554/eLife.23763>.
- Green, S.R., Kragel, P.A., Fecteau, M.E., LaBar, K.S., 2014. Development and validation of an unsupervised scoring system (Automate) for skin conductance response analysis. *Int. J. Psychophysiol.* 91 (3), 186–193. <https://doi.org/10.1016/j.ijpsycho.2013.10.015>.
- Haaker, J., Golkar, A., Hermans, D., Lonsdorf, T.B., 2014. A review on human reinstatement studies: an overview and methodological challenges. In: *Learning & Memory* (Cold Spring Harbor, N.Y.), 21(9), pp. 424–440. <https://doi.org/10.1101/lm.036053.114>.
- Ho, J., Tumkaya, T., Aryal, S., Choi, H., Claridge-Chang, A., 2019. Moving beyond P values: data analysis with estimation graphics. In: *Nature Methods*. <https://doi.org/10.1038/s41592-019-0470-3>.
- Homan, P., Levy, I., Feltham, E., Gordon, C., Hu, J., Li, J., Pietrzak, R.H., Southwick, S., Krystal, J.H., Harpaz-Rotem, I., Schiller, D., 2019. Neural computations of threat in the aftermath of combat trauma. *Nat. Neurosci.* 22 (3), 470–476. <https://doi.org/10.1038/s41593-018-0315-x>.
- Hommel, B., 2009. Action control according to TEC (theory of event coding). *Psychol. Res.* 73 (4), 512–526. <https://doi.org/10.1007/s00426-009-0234-2>.
- Hommel, B., 2011. The Simon effect as tool and heuristic. *Acta Psychol.* 136 (2), 189–202. <https://doi.org/10.1016/j.actpsy.2010.04.011>.
- Hommel, B., 2019. Theory of event coding (TEC) V2.0: representing and controlling perception and action. *Atten. Percept. Psychophys.* 81 (7), 2139–2154. <https://doi.org/10.3758/s13414-019-01779-4>.
- JASP Team, 2020. JASP. In: *Computer software*.
- Kirkpatrick, K., Balsam, P.D., 2016. Associative learning and timing. *Curr. Opin. Behav. Sci.* 8, 181–185. <https://doi.org/10.1016/j.cobeha.2016.02.023>.
- Kuhn, M., Gerlicher, A.M.V., Lonsdorf, T.B., 2022. Navigating the manyverse of skin conductance response quantification approaches – A direct comparison of <sc>trough-to-peak</sc>, baseline correction, and model-based approaches in Ledalab and <sc>PsPM</sc>. *Psychophysiology* 59 (9). <https://doi.org/10.1111/psyp.14058>.
- Lakens, D., 2013. Calculating and reporting effect sizes to facilitate cumulative science: a practical primer for t-tests and ANOVAs. *Front. Psychol.* 4 (1) <https://doi.org/10.3389/fpsyg.2013.00863>.
- Lakens, D., 2022. Sample size justification. *Collabra: Psychol.* 8 (1), 1–31. <https://doi.org/10.1525/collabra.33267>.
- Le Pelly, M.E., 2004. The role of associative history in models of associative learning: a selective review and a hybrid model. In: *Quarterly Journal of Experimental Psychology Section B: Comparative and Physiological Psychology*, Vol. 57, Issue 3, pp. 193–243. <https://doi.org/10.1080/02724990344000141>.
- Li, S.S.-Y., McNally, G.P., 2014. The conditions that promote fear learning: prediction error and Pavlovian fear conditioning. *Neurobiol. Learn. Mem.* 108, 14–21. <https://doi.org/10.1016/j.nlm.2013.05.002>.
- Li, J., Schiller, D., Schoenbaum, G., Phelps, E.A., Daw, N.D., 2011. Differential roles of human striatum and amygdala in associative learning. *Nat. Neurosci.* 14 (10), 1250–1252. <https://doi.org/10.1038/nn.2904>.
- Lonsdorf, T.B., Menz, M.M., Andreatta, M., Fullana, M.A., Golkar, A., Haaker, J., Heitland, I., Hermann, A., Kuhn, M., Kruse, O., Meir Drexler, S., Meulders, B., Nees, F., Pittig, A., Richter, J., Römer, S., Shiban, Y., Schmitz, A., Straube, B., Merz, C.J., 2017. Don't fear 'fear conditioning': methodological considerations for the design and analysis of studies on human fear acquisition, extinction, and return of fear. *Neurosci. Biobehav. Rev.* 77, 247–285. <https://doi.org/10.1016/j.neubiorev.2017.02.026>.
- Mackintosh, N.J., 1974. *The psychology of animal learning*. Academic Press.
- Mackintosh, N.J., 1975. A theory of attention: variations in the associability of stimuli with reinforcement. *Psychol. Rev.* 82 (4), 276–298. <https://doi.org/10.1037/h0076778>.
- Nasser, H.M., Delamater, A.R., 2016. The determining conditions for Pavlovian learning. In: *The Wiley Handbook on the Cognitive Neuroscience of Learning*. John Wiley & Sons, Ltd., pp. 5–46. <https://doi.org/10.1002/9781118650813.ch2>.
- Niv, Y., Schoenbaum, G., 2008. Dialogues on prediction errors. In: *Trends in Cognitive Sciences*, Vol. 12, Issue 7. Elsevier, pp. 265–272. <https://doi.org/10.1016/j.tics.2008.03.006>.
- Niv, Y., Edlund, J.A., Dayan, P., O'Doherty, J.P., 2012. Neural prediction errors reveal a risk-sensitive reinforcement-learning process in the human brain. *J. Neurosci.* 32 (2), 551–562. <https://doi.org/10.1523/JNEUROSCI.5498-10.2012>.
- Pearce, J.M., Hall, G., 1980. A model for Pavlovian learning: variations in the effectiveness of conditioned but not of unconditioned stimuli. *Psychol. Rev.* <https://doi.org/10.1037/0033-295X.87.6.532>.
- Privratsky, A.A., Bush, K.A., Bach, D.R., Hahn, E.M., Cisler, J.M., 2020. Filtering and model-based analysis independently improve skin-conductance response measures in the fMRI environment: validation in a sample of women with PTSD. *Int. J. Psychophysiol.* 158, 86–95. <https://doi.org/10.1016/j.ijpsycho.2020.09.015>.
- Rescorla, R.A., 1988. Pavlovian conditioning: It's not what you think it is. *Am. Psychol.* 43 (3), 151–160. <https://doi.org/10.1037/0003-066X.43.3.151>.
- Rescorla, R.A., Cunningham, C.L., 1979. Spatial contiguity facilitates Pavlovian second-order conditioning. *J. Exp. Psychol. Anim. Behav. Process.* 5 (2), 152–161. <https://doi.org/10.1037/0097-7403.5.2.152>.
- Rescorla, R.A., Wagner, A.R., 1972. A theory of Pavlovian conditioning: variations in the effectiveness of reinforcement and nonreinforcement BT - *Classical conditioning II: current research and theory*. In: *Classical Conditioning II: Current Research and Theory*.
- Rosén, J., Kastrati, G., Åhs, F., 2017. Social, proximal and conditioned threat. *Neurobiol. Learn. Mem.* 142, 236–243. <https://doi.org/10.1016/j.nlm.2017.05.014>.
- Rosén, J., Kastrati, G., Reppel, A., Bergkvist, K., Åhs, F., 2019. The effect of immersive virtual reality on proximal and conditioned threat. *Sci. Rep.* 9 (1), 17407. <https://doi.org/10.1038/s41598-019-53971-z>.
- Serino, A., Noel, J.P., Galli, G., Canzonieri, E., Marmaroli, P., Lissek, H., Blanke, O., 2015. Body part-centered and full body-centered peripersonal space representations. *Sci. Rep.* 5 (November), 1–14. <https://doi.org/10.1038/srep18603>.
- Simon, J.R., Small, A.M., 1969. Processing auditory information: interference from an irrelevant cue. *J. Appl. Psychol.* <https://doi.org/10.1037/h0028034>.
- Society for Psychophysiological Research Ad Hoc Committee on Electrodermal Measures, 2012. Publication recommendations for electrodermal measurements. *Psychophysiology* 49 (8), 1017–1034. <https://doi.org/10.1111/j.1469-8986.2012.01384.x>.
- Starita, F., Lādavas, E., di Pellegrino, G., 2016. Reduced anticipation of negative emotional events in alexithymia. *Sci. Rep.* 6 (1), 27664. <https://doi.org/10.1038/srep27664>.
- Starita, F., Kroes, M.C.W., Davachi, L., Phelps, E.A., Dunsmoor, J.E., 2019. Threat learning promotes generalization of episodic memory. *J. Exp. Psychol. Gen.* 148 (8), 1426–1434. <https://doi.org/10.1037/xge0000551>.
- Starita, F., Garofalo, S., Dalbagno, D., Degni, L.A.E., di Pellegrino, G., 2022. Pavlovian threat learning shapes the kinematics of action. *Front. Psychol.* 13, 6336. <https://doi.org/10.3389/fpsyg.2022.1005656>.
- Starita, F., Pirazzini, G., Ricci, G., Garofalo, S., Dalbagno, D., Degni, L.A.E., Di Pellegrino, G., Magosso, E., Ursino, M., 2023. Theta and alpha power track the acquisition and reversal of threat predictions and correlate with skin conductance response. *Psychophysiology* e14247. <https://doi.org/10.1111/psyp.14247>.
- Stussi, Y., Pourtois, G., Sander, D., 2018. Enhanced Pavlovian aversive conditioning to positive emotional stimuli. *J. Exp. Psychol. Gen.* 147 (6), 905–923. <https://doi.org/10.1037/xge0000424>.
- Stussi, Y., Pourtois, G., Olsson, A., Sander, D., 2021. Learning biases to angry and happy faces during Pavlovian aversive conditioning. *Emotion* 21 (4), 742–756. <https://doi.org/10.1037/emo0000733>.
- Zhang, S., Mano, H., Ganesh, G., Robbins, T., Seymour, B., 2016. Dissociable learning processes underlie human pain conditioning. *Curr. Biol.* 26 (1), 52–58. <https://doi.org/10.1016/j.cub.2015.10.066>.